JANSSEN, T. (1986*b*). *Acta Cryst.* A**42**, 261–271.
JARIĆ, M. V. (1986). *Phys. Rev. B*, **34**, 4685–4698.
KOOPMANS, A., SCHURER, P. J., VAN DER WOUDE, F. & BRONSVELD, P. (1987). *Phys. Rev. B*, **35**, 3005–3008.
KUMAR, V., SAHOO, D. & ATHITHAN, G. (1986). *Phys. Rev. B*, **34**, 6924–6932.
LEVINE, D. & STEINHARDT, P. J. (1986). *Phys. Rev. B*, **34**, 596–616.
LI, X. Z. & KUO, K. H. (1988). *Philos. Mag. Lett.* **58**, 167–171.
PAVLOVITCH, A. & KLÈMAN, M. (1987). *J. Phys. A*, **20**, 687–702.
SCHURER, P. J., VAN NETTEN, T. J. & NIESEN, L. (1988). *J. Phys. (Paris)*, **49**, 237–241.
SOCOLAR, J. E., LUBENSKY, T. C. & STEINHARDT, P. J. (1986). *Phys. Rev. B*, **34**, 3345–3359.
SOCOLAR, J. E. S. & STEINHARDT, P. J. (1986). *Phys. Rev. B*, **34**, 617–647.
STEINHARDT, P. J. (1987). *Mater. Sci. Forum*, **22–24**, 397–408.
STEURER, W. (1987). *Acta Cryst.* A**43**, 36–42.
STEURER, W. & JAGODZINSKI, H. (1988). *Acta Cryst.* B**44**, 344–351.
STEURER, W. & MAYER, J. (1989). *Acta Cryst.* B**45**, 355–359.
YAMAMOTO, A. & ISHIHARA, K. N. (1988). *Acta Cryst.* A**44**, 707–714.

Acta Cryst. (1989). B**45**, 542–549

Structure Refinements of Mg_2TiO_4, $MgTiO_3$ and $MgTi_2O_5$ by Time-of-Flight Neutron Powder Diffraction

BY BARRY A. WECHSLER*

Department of Chemistry, Arizona State University, Tempe, AZ 85287, *USA*

AND ROBERT B. VON DREELE†

*LANSCE, MS H*805, *Los Alamos National Laboratory, Los Alamos, NM* 87545, *USA*

(*Received* 20 *March* 1989; *accepted* 30 *June* 1989)

Abstract

Rietveld refinements using time-of-flight neutron diffraction data are reported for two forms of Mg_2TiO_4 ($M_r = 160{\cdot}51$), $MgTiO_3$ ($M_r = 120{\cdot}20$) and two samples of $MgTi_2O_5$ ($M_r = 200{\cdot}10$). The compounds were synthesized at 1673 K and subsequently annealed and quenched from other temperatures. All data were collected at room temperature on a 10 m powder diffractometer at a nominal scattering angle of 150° 2θ. Mg_2TiO_4 annealed at 973 K has the spinel structure, space group $Fd3m$, with $a = 8{\cdot}4376\ (5)$ Å, $V = 600{\cdot}71\ (11)$ Å^3, $Z = 8$. Mg_2TiO_4 prepared at 773 K is tetragonal, space group $P4_122$, $a = 5{\cdot}9748\ (5)$, $c = 8{\cdot}414\ (7)$ Å, $V = 300{\cdot}37\ (7)$ Å^3, $Z = 4$. Final weighted-profile R values are 0·0376 and 0·0327 for the cubic and tetragonal spinels, respectively. In the cubic form, Mg and Ti are disordered in a single octahedral site to form a nearly perfect inverse spinel, although there may be considerable short-range order. The tetragonal structure is a slight distortion of the cubic one, with two inequivalent octahedral sites over which the Mg and Ti are highly, but completely, ordered. $MgTiO_3$ annealed at 1073 K has the ilmenite structure, space group $R\bar{3}$, $a = 5{\cdot}05478\ (26)$, $c = 13{\cdot}8992\ (7)$ Å, $V = 307{\cdot}56\ (4)$ Å^3, $Z = 6$. The final R_{wp} is 0·0257. Mg and Ti are completely ordered between two octahedral sites, and probably remain so at temperatures up to at least 1673 K. $MgTi_2O_5$ has the pseudobrookite structure, space group $Bbmm$, $Z = 4$. A specimen quenched from 973 K has $a = 9{\cdot}7289\ (9)$, $b = 10{\cdot}0057\ (9)$, $c = 3{\cdot}7416\ (3)$ Å, $V = 364{\cdot}22\ (10)$ Å^3. A second specimen, quenched from 1773 K, has $a = 9{\cdot}7492\ (9)$, $b = 9{\cdot}9896\ (10)$, $c = 3{\cdot}7460\ (4)$ Å, $V = 364{\cdot}82\ (10)$ Å^3. Final R_{wp} are 0·0251 and 0·0230 for the 973 and 1773 K samples, respectively. The Mg–Ti distribution in both samples is disordered, with the 1773 K sample substantially more disordered. The lattice parameters of $MgTi_2O_5$ are sensitive to the degree of disorder. These results have been combined with thermochemical data obtained on the same specimens to derive an understanding of the effects of order–disorder on the phase-stability relations of these compounds.

Introduction

The magnesium titanates Mg_2TiO_4, $MgTiO_3$ and $MgTi_2O_5$ are important as components in industrial ceramics and natural mineral systems. An understanding of the structural variations observed in these compounds and their effects on the stability relations in the system MgO–TiO_2 would be beneficial for estimating properties in more complex systems with related structures. The thermodynamics of these materials has recently been investigated by Wechsler & Navrotsky (1984). In order to characterize the structural state of samples used for thermochemical measurements, we have refined the structures of these compounds.

* Present address: Hughes Research Laboratories, 3011 Malibu Canyon Road, Malibu, CA 90265, USA.
† Author to whom correspondence should be addressed.

0108-7681/89/060542-08$03.00

Mg_2TiO_4 (qandilite) was shown to have the spinel structure, space group *Fd3m*, by Barth & Posnjak (1932). Several subsequent X-ray powder investigations (Agranovskaya & Saksonov, 1966; Okazaki, 1966; De Grave, De Sitter & Vandenberghe, 1975) have confirmed this structure, although the accuracy of these studies is probably not sufficient to rule out the possibility of a small deviation from the completely inverse cation distribution. Delamoye & Michel (1969) reported the transformation of cubic Mg_2TiO_4 to a tetragonal form, space group $P4_122$, after annealing at 753 K for one month. Similar transformations in Mn_2TiO_4 and Zn_2TiO_4 have been studied by X-ray and neutron diffraction (Vincent, Joubert & Durif, 1966; Bertaut & Vincent, 1968). Whereas Mg and Ti are disordered on the single octahedral site in the cubic form, they are ordered into two nonequivalent sites in the tetragonal form. Group-theoretical arguments (Haas, 1965) suggest that the transition must be first order.

$MgTiO_3$ (geikielite) has the ilmenite structure, space group $R\bar{3}$ (Posnjak & Barth, 1934). In this variant of the corundum structure, the cations are ordered into two nonequivalent octahedral sites. Layers of Mg and Ti octahedra alternate along the hexagonal **c** direction. A number of compounds with $A^{2+}B^{4+}O_3$ stoichiometry form the ilmenite structure. At high temperature, a transition to the corundum structure is possible as a result of randomization of the cation distribution. However, this effect has not been demonstrated to occur for any end-member ilmenite at low pressure, although such a transformation is found for ilmenite–corundum solid solutions, *e.g.* intermediate $FeTiO_3$–Fe_2O_3 compositions (Ishikawa, 1958; Burton, 1982). Although the ordering in $MgTiO_3$ has generally been assumed to be complete, no direct determination has previously been reported.

$MgTi_2O_5$ ('karrooite') has the pseudobrookite structure, space group *Bbmm* (Pauling, 1930; Lind & Housley, 1972). The structure consists of bands of edge-sharing octahedra extending in the **b** direction, with the cations occupying two distinct octahedral sites. The distribution of Mg and Ti between the four $M(1)$ and eight $M(2)$ sites per unit cell may vary between normal and inverse arrangements (analogous to the situation in spinel). Several previous studies have addressed the question of cation distribution in $MgTi_2O_5$ and in the isostructural mineral armalcolite ($Fe_{0.5}Mg_{0.5}Ti_2O_5$), of both lunar and synthetic origin, by single-crystal X-ray and Mossbauer techniques (Lind & Housley, 1972; Smyth, 1974; Wechsler, Prewitt & Papike, 1976; Wechsler, 1977; Virgo & Huggins, 1975). These studies suggest that while ordering is essentially complete at low temperatures (in the normal arrangement), substantial cation disorder probably exists at high temperature and is at least partially quenchable. Such findings confirm the prediction of Navrotsky (1975) that $MgTi_2O_5$ and other pseudobrookites are entropy-stabilized phases.

Wechsler & Navrotsky (1984) found that both Mg_2TiO_4 and $MgTi_2O_5$ are stable only at high temperatures because of the configurational entropy arising from cation disorder. Both phases are predicted to be unstable relative to $MgTiO_3$ plus MgO or TiO_2 at low temperatures, although decomposition may be kinetically hindered. The transformation between the cubic and tetragonal forms of Mg_2TiO_4 was found to be associated with very small enthalpy and entropy changes. The entropy change at the transition $\Delta S^0 = 1{\cdot}1\ J\ K^{-1}\ mol^{-1}$, is an order of magnitude smaller than the configurational entropy difference expected on changing from a completely ordered to a completely disordered Mg–Ti octahedral-site distribution. $MgTi_2O_5$ was shown to have lattice parameters that vary continuously with quenching temperature in the range 900–1400 K, presumably as a result of varying cation distribution. Thermochemical data suggest no change in cation ordering in $MgTiO_3$ between 1073 and 1673 K.

Because the thermochemical relations in this system are profoundly influenced by order–disorder properties, structural studies were undertaken to provide constraints for thermochemical models. The primary objectives of the structure refinements reported here were to determine the cation distributions in these materials, to study their dependence on quenching temperature, and to characterize the crystallographic changes accompanying such behavior. Cation distributions determined from early refinements of these data were previously reported by Wechsler & Navrotsky (1984). The site occupancies reported here differ slightly from those values as a result of improved refinement capabilities.

Experimental

Sample preparation

All samples studied were powders synthesized from dried reagent-grade MgO and TiO_2. Mixtures with the appropriate stoichiometry were ground with an agate mortar and pestle under acetone and were heated in a Pt crucible at 1473 K for 48 h in air. Following an intermediate grinding, the powders were heated for an additional 24 h at 1673 K. The sintered products were crushed and ground to pass a 100 mesh sieve. Microscope and X-ray examination revealed that all specimens were single phase.

Before neutron diffraction and thermochemical studies, samples were prepared by annealing portions of the synthesized powders. The cubic spinel was annealed at 973 K for 20 h to simulate the heat

treatments experienced by samples used for solution calorimetry. A tetragonal spinel sample was formed by annealing the Mg_2TiO_4 powder at 773 K for 43 days. $MgTiO_3$ was annealed at 1073 K for 7 days. High- and low-temperature samples of $MgTi_2O_5$ were also prepared by annealing. One sample was annealed at 973 K for 20 h. A second sample was contained in a Pt-foil 'annular'-type capsule and suspended in a vertical tube furnace. After annealing at 1773 K for ~1 h, the sample was drop-quenched into cold water. This sample was light grey in color, in contrast with all the other samples which were slightly off-white. Lattice-parameter measurements of small (~100 mg) samples of $MgTi_2O_5$ that were annealed and quenched from temperatures between 773 and 1773 K (Wechsler & Navrotsky, 1984) suggest that the 973 K sample for neutron diffraction almost certainly has a frozen-in cation distribution corresponding to equilibrium at that temperature. On the other hand, lattice parameters for small samples quenched from 1400 K and above are identical to one another, suggesting that it may not be possible to quench the cation distribution from temperatures in this range. Furthermore, the lattice parameters obtained from X-ray powder patterns of the 1773 K sample used for neutron diffraction indicate that this sample may have a frozen-in distribution corresponding to an equilibrium temperature near 1300 K.

Initially, it was believed that the cubic–tetragonal transformation in Mg_2TiO_4 occurs near 773 K (Delamoye & Michel, 1969). Our experiments before preparation of the neutron diffraction samples showed that superstructure reflections appeared in X-ray diffraction patterns after annealing the cubic phase for two weeks at 773 K. They increased in intensity after an additional two weeks, but no further change was observed in a second month of annealing. Subsequent to the neutron diffraction work, additional experiments were performed that demonstrate that the transition temperature is about 933 ± 20 K. It was also found that annealing at 873 to 903 K for a few days yields material with somewhat sharper, and possibly slightly stronger, superstructure reflections, based on visual observation of X-ray powder patterns. Thus, it is possible that the tetragonal material studied here had not completely reached equilibrium and/or that ordered domains are larger in the material annealed at higher temperatures. Thermochemical studies indicate, however, that tetragonal materials formed at 773 and 873 K are energetically indistinguishable from one another.

Data collection

Intensity data were collected on a 10 m time-of-flight (TOF) resolution focused powder diffractometer at the LANSCE pulsed neutron facility of Los Alamos National Laboratory. Samples (~20 g) were held in a 1 cm diameter by 5 cm long vanadium can. The incident intensity spectrum was measured immediately before the sample runs from a vanadium rod and was fitted to a seven-parameter sum of exponentials. A thin Gd foil was placed in the incident beam to reduce frame overlap from large d-spacing reflections. The diffractometer constant was determined using a standard sample of nickel (a = 3·52387 Å) also examined before the sample runs. The step width was 1·6 μs, and data were collected from 16 counter tubes centered at 150° 2θ for a TOF range 1·800–8·333 ms. The spectra used in the Rietveld refinements were obtained from the 16 individual tube spectra by a binning procedure which compensated for the slight geometric time shift of each spectrum from the mean. The cubic Mg_2TiO_4 sample was subjected to neutrons from $6{\cdot}93 \times 10^6$ proton pulses at 120 Hz, the tetragonal Mg_2TiO_4 sample to $12{\cdot}48 \times 10^6$ pulses in three runs, the $MgTiO_3$ sample to $5{\cdot}94 \times 10^6$ pulses and the quenched $MgTi_2O_5$ sample to $10{\cdot}85 \times 10^6$ pulses. All runs were at room temperature. The proton current was ~3·5 μA during these experimental runs. The total observed profile intensities were subjected to Rietveld analyses as described in the next section.*

Refinement procedures

Rietveld refinements were carried out using the computer program *GSAS* (Larson & Von Dreele, 1986); a summary of the refinement details for all five structures is given in Table 1. The neutron powder peak profiles were modeled with the standard double-exponential Gaussian-convolution function of Von Dreele, Jorgensen & Windsor (1982). The absorption and multiple scattering in the neutron samples were modeled by a wavelength-dependent absorption correction for cylinders (Rouse, Cooper & Chakera, 1970; Hewat, 1979), and the extinction for powders was modeled using the description of Sabine, Jorgensen & Von Dreele (1988). Early refinements of the cubic Mg_2TiO_4 data revealed a considerable amount of oscillating diffuse background. A similar oscillating background was also evident for the two $MgTi_2O_5$ samples but was less pronounced than for cubic Mg_2TiO_4. This background for cubic Mg_2TiO_4 was modeled with a real-space radial distribution consisting of delta functions

$$I_b = C_1 + C_2T + \sum_{i=1}^{n} [C_{i+2}\sin(QR_i)]/QR_i$$

* Lists of observed profile intensities corrected for the incident spectrum, associated estimated standard deviations and positions have been deposited with the British Library Document Supply Centre as Supplementary Publication No. SUP 52156 (69 pp.). Copies may be obtained through The Executive Secretary, International Union of Crystallography, 5 Abbey Square, Chester CH1 2HU, England.

Table 1. *Refinement summaries for magnesium titanates*

Values shown in parentheses are estimated standard deviations in the last place in this and subsequent tables. The values α_1–σ_2^2 are the refined profile coefficients, A and E are absorption and extinction coefficients, respectively.

	Mg_2TiO_4	Mg_2TiO_4	$MgTiO_3$	$MgTi_2O_5$	$MgTi_2O_5$
T_{anneal} (K)	973	773	1073	973	1773
d_{min}	0·370	0·375	0·350	0·480	0·480
N_{obs}	3861	3843	3928	3491	3491
N_{var}	26	29	31	35	35
N_{ref}	352	1844	1749	1038	1063
R_{wp}	0·0376	0·0327	0·0257	0·0251	0·0230
R_p	0·0250	0·0206	0·0163	0·0181	0·0171
χ^2	2·921	2·709	1·820	1·833	1·734
α_1 (μs Å)	0·44 (6)	0·37 (6)	0·46 (6)	0·46 (10)	0·44 (11)
β_0 (μs)	0·0674 (7)	0·0570 (6)	0·0709 (4)	0·0718 (9)	0·0725 (10)
β_1 (μs Å⁴)	0·0050 (2)	0·0047 (2)	0·0032 (1)	0·0027 (3)	0·0027 (3)
σ_0^2 (μs²)	8·4 (9)	8·3 (14)	3·3 (7)	1·5 (18)	−3·5 (27)
σ_1^2 (μs² Å⁻²)	25 (3)	45 (4)	46 (2)	49 (5)	66 (6)
σ_2^2 (μs² Å⁻⁴)	7·1 (12)	1·3 (17)	−1·0 (10)	−2·3 (20)	−4·1 (23)
A	−0·157 (5)	−0·090 (4)	−0·074 (4)	−0·101 (7)	−0·678 (8)
E (μm²)	27 (4)	0	9 (2)	20 (9)	0
$(\Delta/\sigma)_{max}$	0·02	0·03	0·02	0·01	0·06

where T is time of flight, $Q = 2\pi/d$, and C_i and R_i are refinable coefficients. The values of R_i correspond to interatomic vectors in the sample. Backgrounds for the other materials were modeled with three- to eight-term real Fourier sums. The refined values for some of these coefficients for cubic Mg_2TiO_4 are listed in Table 2.

The scattering lengths used for Mg, Ti and O were 0·5375, −0·3438 and 0·5805 ($\times 10^{-12}$ cm), respectively (Koster & Yelon, 1982). In refinements of all samples, a single occupancy parameter was varied, with total site occupancies constrained to stoichiometric values completely describing the Mg–Ti distribution in each case. No disorder was found for $MgTiO_3$ and the result reported here is for the fully ordered structure. In the case of tetragonal Mg_2TiO_4, however, there is a slight uncertainty due to the existence of three distinct cation sites. The possibility of some Ti in the tetrahedral site was tested by allowing the total scattering lengths of the three metal sites to vary without constraint. The result showed that there was less than 1% Ti in the tetrahedral site. Anisotropic temperature factors were refined only in cubic Mg_2TiO_4 and $MgTiO_3$; the others were refined with isotropic temperature factors.

Starting values for atom parameters of cubic Mg_2TiO_4 were taken from the data of Wechsler, Lindsley & Prewitt (1984) on a slightly nonstoichiometric Fe_2TiO_4. The cation distribution was initially assumed to be completely inverse, with Mg and Ti mixed randomly on the octahedral site; the distribution was subsequently refined. Starting atom positions for the tetragonal phase were calculated to make the initial structure identical to that of the cubic phase. Final values of the refined parameters along with the metal—oxygen bond lengths for these two phases are reported in Tables 2 and 3. Final observed and calculated profile intensities and their differences are plotted in Figs. 1 and 2.

Table 2. *Refinement results for cubic* Mg_2TiO_4

	Ti fraction*	x†	U_{11}‡	U_{12}
M(1)	0·002 (3)	⅛	35 (2)	0
M(2)	0·499	½	25 (6)	−3 (4)
O	—	26049 (3)	72 (2)	−18 (1)

Metal—oxygen bond lengths (Å)

M(1)—O	1·9801 (4)	M(2)—O	2·0248 (2)

Radial-distribution distances (Å)§

R_1	1·858 (3)	R_2	2·509 (7)

* Metal-site occupancies constrained so that the total number of metal atoms is fixed and each site is full.

† Atom positions shown × 10^5.

‡ Thermal-motion correction $T = \exp[-2\pi^2(U_{11}h^2a^{*2} + ... + 2U_{12}hka^*b^* + ...)]$. U_{ij} shown as × 10^4 Å².

§ R_1 and R_2 are interatomic distances from radial-distribution background function.

Table 3. *Refinement results for tetragonal* Mg_2TiO_4

	Ti fraction*	x†	y	z	U_{iso}‡
Mg	—	2527 (3)	2527 (3)	⅛	51 (2)
M(1)	0·085 (4)	0	2444 (6)	0	32 (2)
M(2)	0·915	½	2402 (9)	0	32 (4)
O(1)	—	−261 (2)	7377 (3)	2522 (1)	50 (2)
O(2)	—	5182 (2)	2605 (3)	2330 (1)	62 (2)

Metal—oxygen bond lengths (Å)

Mg—O(1)	1·981 (2)	M(1)—O(1)	2·039 (2)	M(2)—O(1)	1·912 (4)
Mg—O(2)	1·986 (2)	M(1)—O(1)	2·093 (1)	M(2)—O(2)	2·038 (4)
		M(1)—O(2)	2·111 (2)	M(2)—O(2)	1·967 (1)

* Metal-site occupancies constrained so that the total number of metal atoms is fixed and each site is full.

† Atom positions shown × 10^4.

‡ Thermal-motion correction $T = \exp[-8\pi^2U_{iso}\sin^2\theta/\lambda^2]$. U_{iso} shown as × 10^4 Å².

Starting values for atom parameters of $MgTiO_3$ were taken from the refinements of $FeTiO_3$ of Wechsler & Prewitt (1984). Final parameter values and M—O bond lengths are given in Table 4 and the profile fit is shown in Fig. 3.

For $MgTi_2O_5$, initial atomic parameters for both samples were taken from the armalcolite data of Wechsler, Prewitt & Papike (1976). Final parameter values and M—O bond lengths for the two samples are given in Tables 5 and 6, and the profile intensities are displayed in Figs. 4 and 5.

Results and discussion

Mg_2TiO_4

Structure refinements confirm that cubic Mg_2TiO_4 has a completely inverse cation distribution (within ±1%). The oxygen positional parameter differs slightly from those reported earlier from X-ray powder data (Table 7). The oxygen thermal ellipsoid is significantly anisotropic, with the maximum displacement (0·095 Å) parallel to the (111) plane. This displacement is comparable to the difference in the ionic radii of Ti^{4+} and Mg^{2+} and thus is probably due to static positional disorder from mixing of Ti and Mg on the octahedral site.

The tetragonal structure is a slight distortion of the cubic one. A small expansion along **a** and contraction along **c** (tetragonal) is observed in the cubic–tetragonal transition for a lattice distortion $(c-a)/a = 0{\cdot}42\%$ with no change in the molar volume. There are two distinct octahedral sites and ordering of Mg and Ti between them is substantial but not complete in the material studied here. The cation-ordering scheme of rows of alternating Mg-rich and Ti-rich sites parallel to **a**. Each site shares edges with six adjacent octahedra so that a Ti-rich site has four Mg-rich sites and two Ti-rich sites as neighbors. The structure is the same as those reported for low-temperature forms of Mn_2TiO_4 and Zn_2TiO_4 (Vincent, Joubert & Durif, 1966; Bertaut & Vincent, 1968) and $(Zn,Co,Ni)_2GeO_4$ (Preudhomme & Tarte, 1980) as well as $ZnLiNbO_4$ (Keramidas, DeAngelis & White, 1975), which is only known to occur in the fully ordered state.

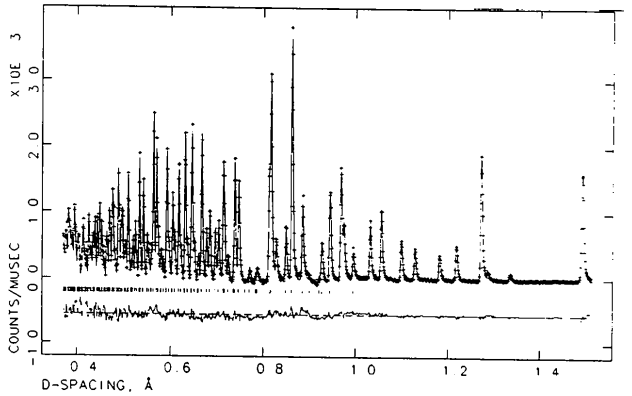

Fig. 1. Observed (+), calculated (−) and difference profiles for cubic Mg_2TiO_4. The background was fitted but has been subtracted from both the observed and calculated profiles for clarity.

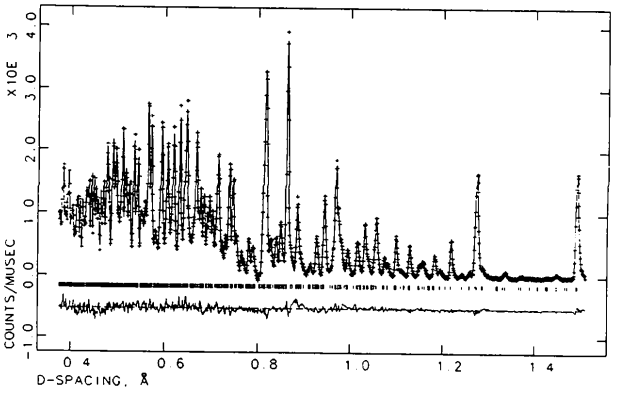

Fig. 2. Observed (+), calculated (−) and difference profiles for tetragonal Mg_2TiO_4. The background was fitted but has been subtracted from both the observed and calculated profiles for clarity.

Table 4. *Refinement results for* $MgTiO_3$

	x^*	y	z	U_{11}†	U_{22}	U_{33}	U_{12}	U_{13}	U_{23}
Mg	0	0	35570 (5)	50 (2)	50 (2)	55 (2)	25 (1)	0	0
Ti	0	0	14510 (7)	35 (2)	35 (2)	42 (3)	18 (1)	0	0
O	31591 (8)	2146 (8)	24635 (3)	40 (2)	41 (2)	59 (2)	16 (1)	10 (1)	13 (1)

Metal—oxygen bond lengths (Å)

Mg—O	2·168 (1)	Ti—O	2·090 (1)
Mg—O	2·047 (1)	Ti—O	1·867 (1)

* Atom positions shown $\times 10^5$.

† Thermal-motion correction $T = \exp[-2\pi^2(U_{11}h^2a^{*2} + \ldots + 2U_{12}hka^*b^* + \ldots)]$. U_{ij} shown as $\times 10^4$ Å^2.

Calorimetric studies of the cubic–tetragonal transition (Wechsler & Navrotsky, 1984) indicate that there is very little difference energetically between the two phases, $\Delta H \cong 1$ kJ mol^{-1}. This is consistent with the relatively subtle structural differences between the two materials. Because the entropy change for this transition must also be very small ($\Delta S = \Delta H/T \cong 1{\cdot}1$ J K^{-1} mol^{-1}) there must be little change in local cation order at the transition temperature. This implies the presence of considerable short-range order in the cubic phase. Many previous studies have also suggested the likelihood of short-range order on the octahedral sites of inverse 2–4 spinels (*e.g.* DeBoer, van Santen & Verwey, 1950; Anderson, 1956; Powell & Powell, 1977; Jacob & Alcock, 1975). For the material studied here the evidence for short-range order might be from the oscillating background in the powder diffraction pattern; however, it could be fitted with just short (1·86 and 2·51 Å) interatomic vectors in a radial-distribution model.

The values of the σ_I^2 profile coefficients for these two phases can be interpreted by an isotropic strain after subtracting an instrument-broadening contribution. The value of σ_I^2 for cubic Mg_2TiO_4 is close to the instrumental value so this sample shows little strain broadening. However, the tetragonal Mg_2TiO_4 has significant strain (~0·1%) which is probably a residual from the cubic–tetragonal phase transition.

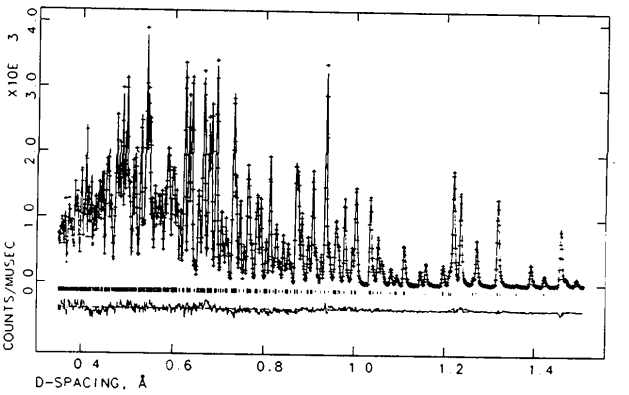

Fig. 3. Observed (+), calculated (−) and difference profiles for $MgTiO_3$. The background was fitted but has been subtracted from both the observed and calculated profiles for clarity.

Table 5. *Refinement results for* 973 K *annealed* $MgTi_2O_5$

	Ti fraction*	x†	y	z	U_{iso}‡
M(1)	0·213 (5)	19521 (22)	¼	0	58 (5)
M(2)	0·894	13255 (16)	56474 (18)	0	35 (3)
O(1)	—	77696 (11)	¼	0	81 (3)
O(2)	—	4606 (8)	11407 (8)	0	82 (3)
O(3)	—	31332 (8)	6499 (8)	0	68 (3)

Metal—oxygen bond lengths (Å)

M(1)—O(1) 2·033 (1)	M(2)—O(1) 2·052 (2)
M(1)—O(2) 1·989 (2)	M(2)—O(2) 1·806 (2)
M(1)—O(3) 2·179 (2)	M(2)—O(2) 1·977 (2)
	M(2)—O(3) 1·944 (1)
	M(2)—O(3) 2·186 (2)

* Metal-site occupancies constrained so that the total number of metal atoms is fixed and each site is full.

† Atom positions shown $\times 10^5$.

‡ Thermal-motion correction $T = \exp[-8\pi^2 U_{iso}\sin^2\theta/\lambda^2]$. U_{iso} shown as $\times 10^4$ Å^2.

Table 6. *Refinement results for* 1773 K *annealed* $MgTi_2O_5$

	Ti fraction*	x†	y	z	U_{iso}‡
M(1)	0·400 (4)	19482 (41)	¼	0	60 (9)
M(2)	0·800	13298 (23)	56108 (25)	0	32 (5)
O(1)	—	77021 (12)	¼	0	112 (4)
O(2)	—	4653 (9)	11521 (8)	0	105 (3)
O(3)	—	31235 (8)	6803 (8)	0	87 (3)

Metal—oxygen bond lengths (Å)

M(1)—O(1) 2·012 (1)	M(2)—O(1) 2·110 (2)
M(1)—O(2) 1·976 (3)	M(2)—O(2) 1·832 (2)
M(1)—O(3) 2·149 (2)	M(2)—O(2) 1·952 (3)
	M(2)—O(3) 1·949 (1)
	M(2)—O(3) 2·173 (3)

* Metal-site occupancies constrained so that the total number of metal atoms is fixed and each site is full.

† Atom positions shown $\times 10^5$.

‡ Thermal-motion correction $T = \exp[-8\pi^2 U_{iso}\sin^2\theta/\lambda^2]$. U_{iso} shown as $\times 10^4$ Å^2.

Neither sample showed significant crystallite-size broadening (σ_2^2 is close to zero); in fact the extinction coefficient for the cubic phase indicates an average crystallite size of ~5 μm. No extinction was observed for tetragonal Mg_2TiO_4 so the crystallite size is in the range 0·1–1 μm.

$MgTiO_3$

The refined structure of $MgTiO_3$ is virtually identical to that of $FeTiO_3$ (Wechsler & Prewitt, 1984); the slight differences may be ascribed primarily to the smaller size of the Mg^{2+} cation relative to Fe^{2+}. The distribution of Mg and Ti over the two octahedral sites is found to be completely ordered. Together with calorimetric evidence indicating no enthalpy difference between $MgTiO_3$ quenched from 1673 K and that quenched from 1073 K, these results argue strongly that this distribution is retained at high temperature, consistent with observations made for other isostructural compounds. As with the tetragonal Mg_2TiO_4, the value of the σ_1^2 profile coefficient indicates some residual strain (~0·1%) in this sample. Its origin is unknown because the material is apparently completely ordered and unlike Mg_2TiO_4 there is no phase transition. The extinction coefficient gives an average crystallite size of ~3 μm.

$MgTi_2O_5$

In contrast with $MgTiO_3$, the Mg–Ti distribution in $MgTi_2O_5$ is highly disordered. Defining the inversion parameter, α, to be the fraction of Ti in the $M(1)$ site, a statistically random Ti–Mg distribution would have $\alpha = \frac{2}{3}$. Thus, the sample quenched from 1773 K has a distribution approaching complete inversion but is not completely inverted. The 973 K sample, while approaching the normal ordered distribution, is still significantly disordered. An earlier single-crystal X-ray refinement of synthetic $MgTi_2O_5$ annealed at 1773 K (Lind & Housley, 1972) gave a value intermediate to the distribution determined here, $\alpha = 0{\cdot}316$. Their sample, however, was not quenched and therefore would be expected to be more highly ordered than our 1773 K sample, as is observed.

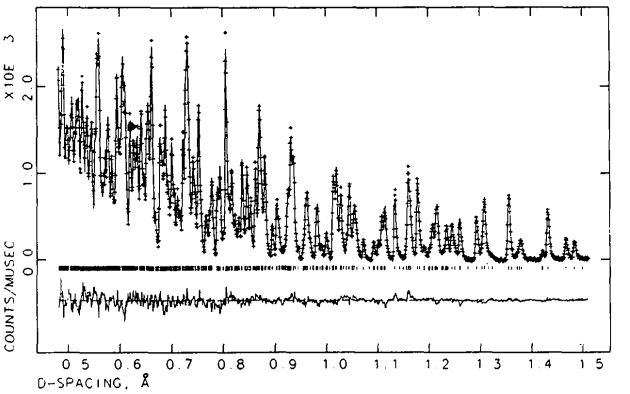

Fig. 4. Observed (+), calculated (−) and difference profiles for $MgTi_2O_5$ quenched from 973 K. The background was fitted but has been subtracted from both the observed and calculated profiles for clarity.

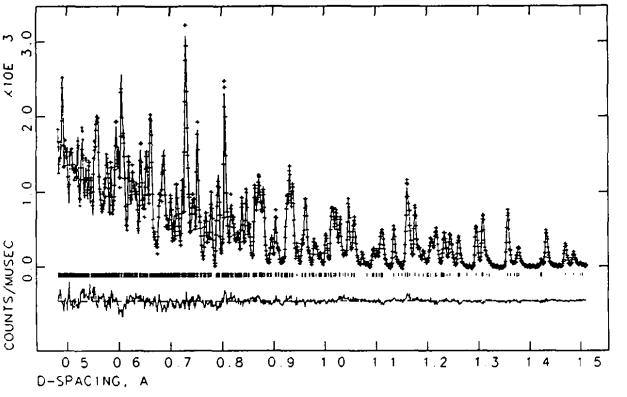

Fig. 5. Observed (+), calculated (−) and difference profiles for $MgTi_2O_5$ quenched from 1773 K. The background was fitted but has been subtracted from both the observed and calculated profiles for clarity.

Table 7. *Reported oxygen positional parameters for cubic* Mg_2TiO_4

u*	Reference
0·265 (6)	Barth & Posnjak (1932)
0·262 (3)	Agranovskaya & Saksonov (1966)
0·2625 (5)	Okazaki (1966)
0·265 (1)	De Grave, De Sitter & Vandenberghe (1975)
0·26049 (3)	This work

* Referred to choice of origin at center of symmetry.

The experiments of Wechsler & Navrotsky (1984) showed a continuous variation in lattice parameters of $MgTi_2O_5$ with quenching temperature, with an overall volume increase of about 0·2% over the temperature range 773–1773 K. This effect is clearly reflected in the refined lattice parameters determined here. Similar trends have been reported for armalcolite (Wechsler, Prewitt & Papike, 1976; Wechsler, 1977). These observations suggest that the cation distribution is also continuously variable. Although lattice parameters of samples quenched from temperatures above 1400 K are essentially constant, high-temperature X-ray and calorimetric measurements by Brown & Navrotsky (1989) strongly suggest that cation disorder in $MgTi_2O_5$ continues to increase at higher temperatures, becoming essentially random above 1800 K. However, this disorder is not quenchable above ~1400 K. The inversion parameter determined for our 1773 K sample is therefore probably representative of the temperature at which the disorder was frozen in (probably near 1300 K, as noted above), whereas the results for the 973 K sample are probably indicative of the equilibrium distribution at that temperature.

Mean $M(1)$—O and $M(2)$—O distances also reflect the difference in ordering between the high- and low-temperature samples. In addition, the isotropic temperature factors of the oxygen atoms are higher in the high-temperature sample, suggesting greater positional disorder resulting from the more-disordered cation distribution.

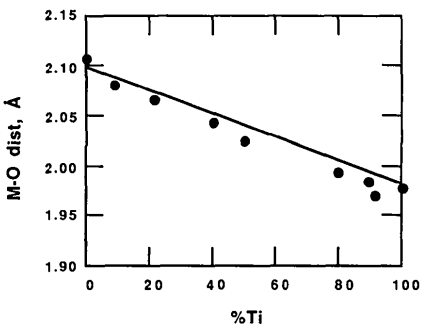

Fig. 6. Mean metal—oxygen distances for octahedral sites in magnesium titanates. Values observed in this work are shown as solid circles and the line is drawn between the Mg—O and Ti—O distances from the ionic radii of Shannon & Prewitt (1969).

The combination of cation-distribution data with calorimetrically measured enthalpy effects allows one to model the thermodynamics associated with cation disorder. Although an uncertainty arises owing to the possibility that the cation distribution of our sample quenched from 1773 K is not representative of the equilibrium distribution at that temperature, it is nevertheless possible, using the 'simple equilibrium' model of Navrotsky & Kleppa (1967), to estimate that the interchange enthalpy is about 27 ± 2 kJ mol^{-1} (Wechsler & Navrotsky, 1984). This value is of the same order as $T\Delta S_{conf}$, accounting for the tendency towards cation disorder at high temperature.

Comparing the σ_1^2 profile for the two samples of $MgTi_2O_5$ indicates that there is some strain in both samples with more in the material quenched from the higher temperature (~0·14 *vs* ~0·11%). This strain is probably induced by the 'frozen-in' cation disorder in each sample. Both samples show no particle-size broadening of the diffraction lines. The 973 K sample shows an extinction effect from a crystallite size of ~5 μm.

Metal–oxygen bond lengths

Of the eleven metal sites observed in the five structures examined by this study, nine are octahedral and they exhibit Ti fractions ranging from 0 to 1. In Fig. 6 the mean M—O distance *vs* Ti fraction is plotted for all nine octahedra. As can be seen, there is a small negative deviation from Vegard's law for mixing Mg and Ti on these sites. Thus, there might be a slight tendency to greater disorder in these magnesium titanates at higher pressure owing to this nonideal behavior. This nonideality appears to have little or no effect on the temperature dependence of the disordering since the thermodynamic measurements suggest that the disorder is primarily entropy driven at atmospheric pressure.

This work was performed under the auspices of the US Department of Energy and funded in part by its Office of Basic Energy Sciences, Division of Materials Sciences.

References

AGRANOVSKAYA, A. I. & SAKSONOV, YU. G. (1966). *Sov. Phys. Crystallogr.* **11**, 196–198.
ANDERSON, P. W. (1956). *Phys. Rev.* **102**, 1008–1013.
BARTH, T. F. W. & POSNJAK, E. (1932). *Z. Kristallogr. Teil A*, **82**, 325–341.
BERTAUT, E. F. & VINCENT, H. (1968). *Solid State Commun.* **6**, 269–275.
BROWN, N. E. & NAVROTSKY, A. (1989). *Am. Mineral.* **74**, 902–912.
BURTON, B. (1982). PhD Thesis, State Univ. of New York, USA.
DEBOER, F., VAN SANTEN, J. H. & VERWEY, E. J. W. (1950). *J. Chem. Phys.* **18**, 1032–1034.

DE GRAVE, E., DE SITTER, J. & VANDENBERGHE, R. (1975). *Appl. Phys.* **7**, 77–80.
DELAMOYE, P. & MICHEL, A. (1969). *C. R. Acad. Sci. Ser. C*, **269**, 837–838.
HAAS, C. (1965). *J. Phys. Chem. Solids*, **26**, 1225–1232.
HEWAT, A. W. (1979). *Acta Cryst.* A**35**, 248–250.
ISHIKAWA, Y. (1958). *J. Phys. Soc. Jpn*, **13**, 828–837.
JACOB, K. T. & ALCOCK, C. B. (1975). *High Temp. High Pressures*, **7**, 433–439.
KERAMIDAS, V. G., DEANGELIS, B. A. & WHITE, W. B. (1975). *J. Solid State Chem.* **15**, 233–245.
KOSTER, L. & YELON, W. B. (1982). *Neutron Diffraction Newsletter*. ECN Netherlands Energy Research Foundation, Petten, The Netherlands.
LARSON, A. C. & VON DREELE, R. B. (1986). *GSAS – Generalized Structure Analysis System*. Report LA-UR 86-748. Los Alamos National Laboratory, New Mexico, USA.
LIND, M. D. & HOUSLEY, R. M. (1972). *Science*, **175**, 521–523.
NAVROTSKY, A. (1975). *Am. Mineral.* **60**, 249–256.
NAVROTSKY, A. & KLEPPA, O. J. (1967). *J. Inorg. Nucl. Chem.* **29**, 2701–2714.
OKAZAKI, H. (1966). *Jpn J. Appl. Phys.* **5**, 559–560.
PAULING, L. (1930). *Z. Kristallogr.* **73**, 97–112.
POSNJAK, E. & BARTH, T. F. W. (1934). *Z. Kristallogr. Teil A*, **88**, 271–280.
POWELL, R. & POWELL, M. (1977). *Mineral. Mag.* **41**, 257–263.
PREUDHOMME, J. & TARTE, P. (1980). *J. Solid State Chem.* **35**, 272–277.
ROUSE, K. D., COOPER, M. J. & CHAKERA, A. (1970). *Acta Cryst.* A**26**, 682–691.
SABINE, T. M., JORGENSEN, J.-E. & VON DREELE, R. B. (1988). *Acta Cryst.* A**44**, 374–379.
SHANNON, R. D. & PREWITT, C. T. (1969). *Acta Cryst.* B**25**, 925–946.
SMYTH, J. R. (1974). *Earth Planet. Sci. Lett.* **24**, 262–270.
VINCENT, H., JOUBERT, J. C. & DURIF, A. (1966). *Bull. Soc. Chim. Fr.* pp. 246–250.
VIRGO, D. & HUGGINS, F. E. (1975). *Carnegie Inst. Washington Yearb.* **74**, 585–590.
VON DREELE, R. B., JORGENSEN, J. D. & WINDSOR, C. G. (1982). *J. Appl. Cryst.* **15**, 581–589.
WECHSLER, B. A. (1977). *Am. Mineral.* **62**, 913–920.
WECHSLER, B. A., LINDSLEY, D. H. & PREWITT, C. T. (1984). *Am. Mineral.* **69**, 754–770.
WECHSLER, B. A. & NAVROTSKY, A. (1984). *J. Solid State Chem.* **55**, 165–180.
WECHSLER, B. A. & PREWITT, C. T. (1984). *Am. Mineral.* **69**, 176–185.
WECHSLER, B. A., PREWITT, C. T. & PAPIKE, J. J. (1976). *Earth Planet. Sci. Lett.* **29**, 91–103.

Acta Cryst. (1989). B**45**, 549–555

Charge Density of FeF_2

BY M. J. M. DE ALMEIDA, M. M. R. COSTA AND J. A. PAIXÃO

Centro FC1, INIC, Department of Physics, University of Coimbra, 3000 Coimbra, Portugal

(*Received* 14 *September* 1988; *accepted* 17 *July* 1989)

Abstract

The electron density distribution of a rutile-type structure, FeF_2, has been derived from X-ray diffraction measurements carried out on two single crystals at room temperature. Difference density maps were calculated using atomic and temperature parameters refined from high-angle data with $(\sin\theta)/\lambda \geq 0{\cdot}6$ Å^{-1}. The electron populations of $3d$ orbitals were obtained from a least-squares refinement, using model and observed $3d$ structure factors. A comparison is made between these and the results of a multipole refinement. Crystal data: FeF_2, $M_r = 93{\cdot}84$, tetragonal, $P4_2/mnm$, $a = 4{\cdot}7000\ (4)$, $c = 3{\cdot}3100\ (3)$ Å, $V = 73{\cdot}12$ Å^3, $Z = 2$, $D_x = 4{\cdot}2622$ Mg m^{-3}, λ(Mo $K\alpha$) = 0·7017 Å, μ(Mo $K\alpha$) = 49·3 cm^{-1}, $F(000) = 88$, room temperature. Final R values (spherical refinement): 0·010 for 170 reflections from crystal A, 0·012 for 157 reflections from crystal B.

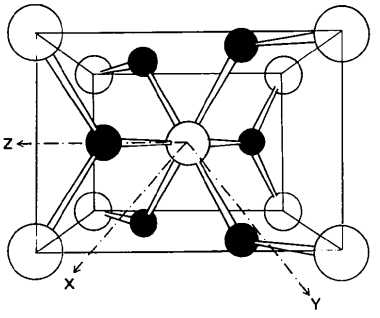

Fig. 1. Unit cell of the rutile structure, showing the directions of the set of axes used in the analysis of $3d$-orbital populations. The open circles represent the positions of Fe atoms and the filled circles those of F atoms.

Introduction

In recent years, several rutile-type structures, MF_2, where M is a transition-metal atom (see Fig. 1), have been examined in our laboratory.

Electrons in the partially filled $3d$ shell of the transition metal 'see' a strong crystal field with a particular symmetry. Consequently, some of the $3d$ orbitals are preferentially occupied, resulting in an aspherical density distribution around the metal atom.

0108-7681/89/060549-07$03.00